J Mater Sci: Mater Med (2008) 19:1775–1785
DOI 10.1007/s10856-007-3331-z

PLD bioactive ceramic films: the influence of $CaO–P_2O_5$ glass additions to hydroxyapatite on the proliferation and morphology of osteblastic like-cells

Gisela Marta Oliveira · Maria P. Ferraz · Pío G. González · Julia Serra · Betty Leon · Mariano Pèrez-Amor · Fernando J. Monteiro

Received: 25 October 2006 / Accepted: 19 November 2007 / Published online: 6 December 2007

Abstract This work consists on the evaluation of the in vitro performance of Ti6Al4V samples PLD (pulsed laser deposition) coated with hydroxyapatite, both pure and mixed with a $CaO–P_2O_5$ glass. Previous studies on immersion of PLD coatings in SBF, showed that the immersion apatite films did not present the usual cauliflower morphology but replicated the original columnar structure and exhibited good bioactivity. However, the influence of glass associated to hydroxyapatite concerning adhesion, proliferation and morphology of MG63 cells on the films surface was unclear. In this study, the performance of these PLD coated samples was evaluated, not only following the physical–chemical transformations resulting from the SBF immersion, but also evaluating the cytocompatibility in contact with osteoblast-like MG63 cells. SEM and AFM confirmed that the bioactive ceramic PLD films reproduce the substrate's surface topography and that the films presented good adherence and uniform surface roughness. Physical–chemical phenomena occurring during immersion in SBF did not modify the original columnar structure. In contact with MG63 cells, coated samples exhibited very good acceptance and cytocompatibility when compared to control. The glass mixed with hydroxyapatite induced higher cellular proliferation. Cells grown on these samples presented many filipodia and granular structures, typical features of osteoblasts.

G. M. Oliveira · M. P. Ferraz · F. J. Monteiro
Laboratório de Biomateriais, INEB - Instituto de Engenharia Biomédica, Rua do Campo Alegre 823, 4150-180 Porto, Portugal

G. M. Oliveira (✉) · M. P. Ferraz
Universidade Fernando Pessoa, Praça Nove de Abril 349, 4249-004 Porto, Portugal
e-mail: gisela@ufp.pt

P. G. González · J. Serra · B. Leon · M. Pèrez-Amor
Departamento de Física Aplicada, Universidad de Vigo, Lagoas, Marcosende, 9, 36280 Vigo, Spain

F. J. Monteiro
Departamento de Engenharia Metalúrgica e de Materiais, Faculdade de Engenharia, Universidade do Porto, Rua Dr. Roberto Frias, 4200-465 Porto, Portugal

1 Introduction

Application of implants and prostheses is a frequent clinical procedure to repair dental and bone defects [1–3]. Biomaterials used in these biomedical devices have to be biocompatible, ensuring the biological function of substituting tissues or organs and also providing osteoconduction and osteointegration.

Experience accumulated over the past few decades has led to development of implants made of highly resistant metals (usually titanium or its alloy) which are able to withstand high loads as it is the case for the majority of bones, coated with ceramic materials like hydroxyapatite, bioactive glasses or associations of these materials [4, 5]. Hydroxyapatite (HA) has been extensively used in coating due to its bioactivity and bonding to living bone tissue. The rapid attachment of osteoblasts onto the implant HA surface (osteogenesis) and subsequent vascularization and mineralization is the mechanism thought to be responsible for implant success [6–8].

Although hydroxyapatite is chemically very similar to the extracellular bone matrix (ECM), it is at present, recognised as having limited bioactivity mainly due to its almost insoluble behaviour in physiological media. This is the reason attributed for slow osteointegration process

(inducing prolonged post-surgical recovering times). On the other side, bioactive glasses containing SiO_2, have demonstrated accelerated biodegradation and re-absorption in the physiological environment also leading to prostheses failure.

Researchers have been proposing new associations of biomaterials and different surface treatments attempting to increase the life-time of prosthesis through strong adherence to the host bone, resulting from osteoconduction ability of these biomaterials.

Previous experimental work [9–12], has shown that reaction of HA with low quantities (2–5% in weight) of glasses from the $CaO–P_2O_5$ system could improve mechanical properties of HA coatings, especially fracture toughness. Furthermore, the mixture of these glasses with synthetic HA incorporates chemical species such as Na^+, K^+, Mg^{2+} and F^- or PO_4^{3-} ions known to substitute (respectively) Ca^{2+} and CO_3^{2-} ions in bone apatite.

At present, the plasma-spray technique [13] is the best commercially available technical process to produce coatings for implants. However, the clinical success of the rehabilitation expected by the application of plasma-spray coated implants is questioned by acute inflammatory reactions, that may lead to a new surgery to substitute the first implant [14]. These unsuccessful situations are, most frequently, attributed to the chemical or mechanical degradation of the coating (during plasma-spray processing) and its decreased adherence to the metallic substrate [15]. The de-lamination of the thick plasma-spray coatings has also been observed on implants of patients submitted to a revising surgery.

As an alternative to plasma-spray, the use of the PLD technique to coat biomedical devices is, still under research. Previous studies [16] indicate that this technique may represent a possible solution in some cases of the above referred plasma-spray difficulties. The PLD process presents several advantages over the plasma-spraying technique: PLD coatings produce extremely thin films (generally less than 2 μm thick), with a regular surface topography, showing excellent adhesion to the substrate, chemical stability and reduced surface roughness.

The objective of this work was to evaluate the in vitro bioactivity and cytocompatibility of PLD coatings of hydroxyapatite and hydroxyapatite +1.5% bioactive glass mixtures on titanium alloy substrates in contact with MG63 osteoblast-like cells.

2 Materials and methods

2.1 PLD samples preparation

Synthetic, crystalline, highly pure and biomedical application grade hydroxyapatite (HA) $Ca_{10}(PO_4)_6(OH)_2$ was obtained from *Plasma Biotal Ltd.* (Tideswell, UK). A $P_2O_5–CaO$ glass (BG) containing 35, 35, 20 and 10 mol% of P_2O_5, CaO, Na_2O and K_2O, respectively, was prepared as previously described [17].

A mixture of 1.5% (in weight) $P_2O_5–CaO$ glass with pure hydroxyapatite was prepared according to Ferraz et al. [12] and used for targets. Commercially available Ti6Al4V alloy (Thyssen, Hannover, Germany) was used as substrate in 20 × 15 mm pieces of rectangular shape and 6 mm diameter disks, both with 2 mm thickness. The PLD coating technique was described elsewhere [18–22]. Coatings were produced at 460 °C in a reactive atmosphere of water vapour, at constant pressure of 0.45 mbar, with the focussed ArF laser beam (193 nm) operating at 10 Hz and 200 mJ/pulse.

2.2 SBF immersion tests

Following previous work [12], two groups samples (HA and HA + 1.5%BG) were immersed in 50 mL of Simulated Body Fluid (SBF) solution [23], at 37 °C, with controlled orbital agitation and for time periods of 8, 16 and 48 h, with no solution refreshments. Three replicates used for each group and immersion period. After immersion, samples were dried at room temperature and selected for surface analysis by XPS, AFM, XRD and SEM/EDS.

XPS analyses were performed in a VG ESCALAB 200 A equipment with 300 W power and with an energy of 50 eV for the general spectra (surveys) and of 20 eV for specific element peak spectra. Aliphatic carbon peak (C1s), with a corresponding energy of 285.0 eV was used as a reference for correction of other peaks positions (corresponding to other elements binding energy). XPS data acquired in ASCII format were fitted and analysed using the XPS PEAK software, version 4.1.

In order to expose the cross section of the coating and under layers, samples immersed in SBF solution were mechanically bent at an approximate angle of 10°, in the longitudinal direction.

Samples submitted to contact with cells were aseptically processed and dehydrated as follows: all samples were gold sputtered using a JEOL JFC 1100 equipment before SEM observation.

A JEOL JSM-6301F scanning electron microscope was used, operating at 15 mm working distance, variable magnification between 250 and 10,000 times and 5–7 keV energy. Images were acquired under secondary electrons mode and registered in digital format. X-ray dispersive energy microanalysis (EDS) was performed with a Pioneer 6301F spectrometer.

Finally, the surface topography evaluation was performed using an Atomic Force Microscope (AFM)

TopoMetrix system (Discoverer) using a contact mode sensor. A 100 μm scanner was used to obtain 80 × 80 μm surveys. Average roughness Ra (centre line average or mean value of the surface height relative to the centre plane) and Rms (mean square value of roughness) values were calculated.

2.3 Cell culture

PLD coated discs of 6 mm diameter used for cytocompatibility tests underwent dry heat sterilization in an oven at 160 °C, at atmospheric pressure for 2 h. Immediately after sterilization and before cell incubation, discs were aseptically transferred to 96-well polystyrene culture plates.

Cytocompatibility tests were performed using MG63 cells, an immortalized, very well characterized and cryogenically preserved osteoblastic precursor cell line. After de-frosting of a cryopreserved vial, sub-cultures of this cell line were maintained in Minimum Essential Medium α-MEM (enriched with 10% (v/v) FBS, 0.5% gentamicin and 1.0% fungizone) in 75 mL polystyrene animal cell culture flasks, and incubated at 37 °C in 5.0% (v/v) CO_2 in humid atmosphere. When achieving confluence, cells were washed with PBS (phosphate buffered saline), harvested with trypsin in EDTA, and re-suspended in fresh culture media, at 37 °C. Aliquots diluted with trypan blue were used for calculation of cell concentration at the optical microscope, using a Neubauer counting chamber.

After cell suspension dilution, cells were incubated into non-treated polystyrene 96-well plates, deposited onto the PLD coated surface of the discs (using 50 μL of suspension per disc) of a 6.44 (±0.41) × 10^4 cells/mL suspension. After two hours incubation to allow cell adherence, 150 μL of fresh α-MEM medium was added to each well. Two sets of forty PLD coated discs (one set HA coated and other HA + 1.5%BG coated) were used in each experiment. As control, the non-treated PS surface of the culture plates was used: in each 96-well plate, 5 wells were inoculated as previously described.

Cells were allowed to incubate with tested materials at different contact times: zero (corresponding to only 2 h for adherence); 2 days (48 h); 4 days (96 h) and 8 days in the same previously referred conditions. For each incubation time, two 96 well plates were used each containing five replicates for MTT (methylthiazol tetrazolium, Sigma M5655) test, three replicates for DNA test and two replicates for SEM observation, of each group of the tested material: both HA and HA + 1.5%BG coated samples. At every 2 days culture medium was discharged and replaced.

After the incubation periods, plates were removed from the incubating chamber and samples were aseptically processed for test.

2.3.1 Cell proliferation

At the end of each contact time, three replicates of each group of samples were used for DNA determination with the bis-benzimide (Hoechst 33258) method, using a Varian Cary Eclipse fluorescence spectrometer. In the incubating plate, culture medium was discarded, samples rinsed with PBS and aseptically transferred to a new plate. About 80 μL 1% Triton solution was added to each sample and the plate submitted to orbital agitation at 4 °C for 1 h. Samples were preserved at −21 °C until analysis and then de-frosted at 4 °C. From each disc sample, three aliquots (20 μL each) of cell lysate were taken for analysis. About 1% Triton solution was used as blank correction and calibration curves were constructed using both MG63 suspensions of known cell concentrations and a calf thymus DNA standard solution.

2.3.2 Cell viability

Immediately after concluding these contact periods, five replicates of each group of samples were taken for MTT testing. Culture medium was discarded; samples were rinsed with PBS and aseptically transferred to a new plate. About 15 μL of MTT reagent and 150 μL of α-MEM medium were added to each sample disc and plates were incubated for 3 h at 37 °C. Formazan crystals (obtained by cleavage of MTT by mitochondrial activity of viable cells) were dissolved in DMSO and absorbance measured in a SLT Spectra plate spectrometer. Calibration curves were constructed using MG63 suspensions of known cell concentrations in α-MEM medium.

2.3.3 Cell morphology

At the end of each contact period, two replicates of each coating group, were harvested from culture media, rinsed with PBS solution and transferred to a 1.5% glutaraldehyde solution buffered (pH 7.3) in sodium cacodylate 0.14 M for 30 min. After cells fixation, discs were washed with distilled water and de-hydrated by immersion in ethanol solutions of growing concentrations from 50 to 99.8%, with a residence time of 10 min in each ethanol solution. After de-hydration, cells were dried to critical point.

Scanning electron microscope observation was performed under the previously described conditions, at variable magnification between 20 and 5,000× and 10 keV energy. Images were acquired under backscattered and secondary electrons modes.

All data present in the results were calculated based on the mean of reproducible results of replicates (results

beyond 90% confidence were disregarded). Means and standard deviations were calculated using Microsoft 'Excel'. Hypothesis tests on differences between means of small dimension samples (*t*-tests with 0.05 confidence level) were applied for comparison of results.

3 Results

3.1 SBF immersion tests

3.1.1 SEM

PLD films presented uniform surfaces and mechanical stress applied to bend the samples up to 10° was not strong enough to break the film and expose the cross section without damaging the surface (Fig. 1).

For the samples immersed for 16 and 48 h, the applied stress (resulting from mechanical bending) broke the film, producing transversal small cracks and lifting the upper layers, exposing the zones underneath the top layer. In Fig. 1 (right) it may be observed that, the PLD film was extremely adherent to the substrate (underneath the exposed layer remained a stacked ceramic layer, which composition was confirmed by EDS analysis). The detached layer of the coating reveals, as expected, a very compact, homogeneous columnar structure as found in previous work [12, 24]. This compact microstructure of rounded columns extends vertically from the under layer to the surface of the film terminating with domed tops contributing to the surface roughness. No morphologic differences could be detected between the two different groups of coatings, indicating that this typical columnar structure was independent of the coating chemical composition. The under layer stacked to the substrate could be observed in all samples (both HA and HA + 1.5%BG) immersed in SBF for longer periods (16 and 48 h).

SEM observation of the exposed coating layers also allowed for measurements of the cross section thickness. Results are presented in Fig. 2.

The values in Fig. 2 represent only the thickness of the exposed cross section layers and not the total film thickness. HA + 1.5%BG exposed layers were thicker than HA.

3.1.2 AFM

AFM topographic images confirm the morphology observed by SEM analysis, but it is only possible to observe the surface constituted by the domed tops of the columnar structure (Fig. 3). Aligned grooves resulting from the columnar compaction and orientation are also observable. Topographic images obtained by AFM analysis revealed that, before SBF immersion, HA PLD coated surfaces generally present larger globules than the HA + 1.5%BG coatings.

Ra and Rms values calculated for these PLD coatings were 0.51 ± 0.12 μm and 0.63 ± 0.13 μm (respectively) and are presented in Table 1, together with references found in literature, for comparison.

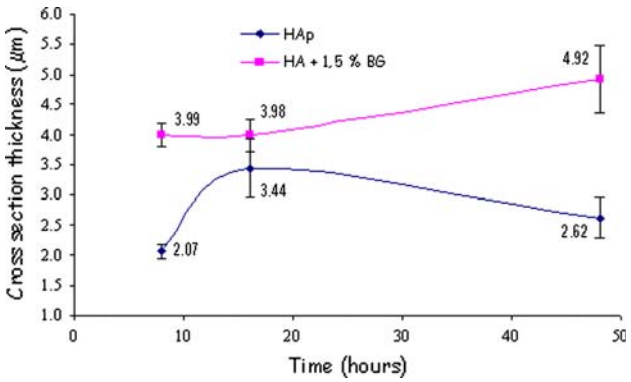

Fig. 2 Cross section thickness variation with immersion time in SBF solution of detached exposed layers of the PLD coatings

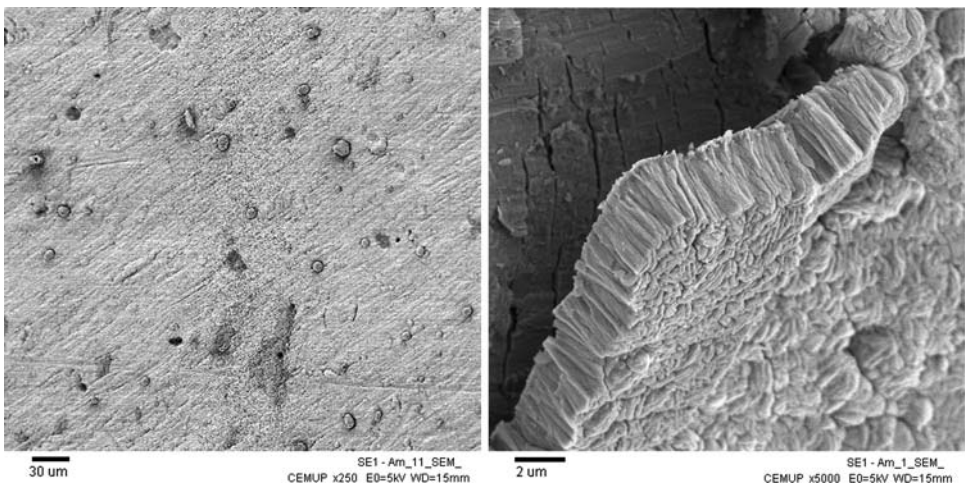

Fig. 1 Surface of a HA PLD coating after 8 h (left) and after 16 h (right) immersion in SBF solution (magnification 250× and 5000×; energy 5 KV)

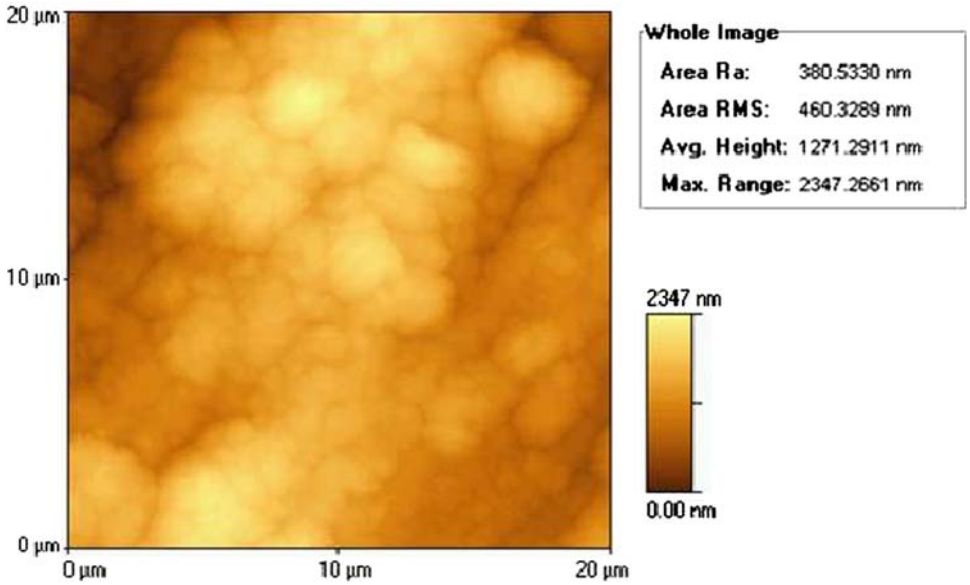

Fig. 3 AFM image of PLD HA + 1.5%BG coating after 48 h SBF immersion

However, immersion in SBF inverted the situation transforming the HA + 1.5%BG coating in a rougher surface than the HA coating. HA film surface is more compact and the size of the globules is smaller, corresponding to lower roughness. However, on the original films before SBF immersion, HA presented larger grain size. Probably these differences can be attributed to an increased accumulation of precipitate on the HA + 1.5% BG surface during immersion in SBF, which is also in agreement with the thicker cross sections found for these films.

3.1.3 XPS

The chemical composition of the films top surfaces were studied by XPS analysis before and after immersion in SBF solution. As expected, six elements were detected: calcium, carbon, magnesium, oxygen, phosphorous and sodium. With the exception of sodium, the other elements atomic composition was statistically similar for HA and HA + 1.5%BG, when comparing the same immersion period (results not shown). The evolution of the Ca/P ratio (commonly used for characterizing CaP compounds) with SBF immersion time, expressed in terms of values obtained by XPS analyses are presented in Fig. 4. The values presented in the graph are average values of XPS and EDS results.

Although the initial Ca/P ratio is different for HA and HA + 1.5%BG original coatings (and both higher than the theoretical 1.67) they became statistically similar after 8 h of immersion, stabilizing at 1.4, as a consequence of simultaneously diminishing the calcium atomic percentage at the surface and increasing of the phosphorous content. Remarkably, natural bone apatite has Ca/P of 1.49, very close to the values obtained for the PLD SBF immersion films. These results were confirmed by EDS analysis.

Table 1 Average roughness (Ra) values for tested PLD coatings and other HA or Ti surfaces treated for biomaterial purposes

Biomaterial surface treatment	Average roughness Ra (µm)
HA PLD tested samples[a]	0.51 ± 0.12
Pre-treated pure titanium	0.54 ± 0.20 [25]
	0.60 ± 0.02 [26]
PLD	0.30 [27]
HA plasma-sprayed	3.60 ± 0.16 [28]
	2.07 ± 0.36 [29]

[a] Measured by AFM analysis

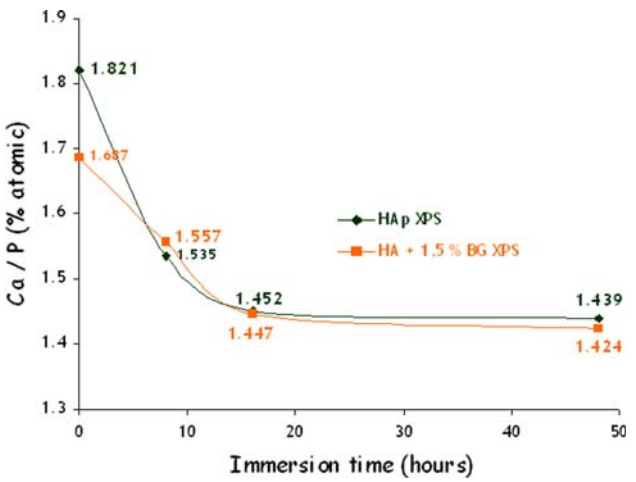

Fig. 4 Ca/P ratio variation with SBF immersion time

3.1.4 XRD

XRD analysis supported the results obtained by XPS: HA and HA + 1.5%BG spectra shown in Fig. 5 follow the same pattern. Besides hydroxyapatite, the presence of β-TCP and CaO (this later expected in the glass containing coating) are detected by reflexions 210 and 214 (for β-TCP) and 200 and 211 (for CaO). The presence of these substances in hydroxyapatite PLD coatings has been reported in previous works [16, 30] as a consequence of the coating technique itself.

3.2 Cytocompatibility assessment

In Fig. 6 the total area of the discs tested in contact with MG63 cells may be observed. Only after 8 days of contact, cells reached confluence and for early times they can be observed only in restricted areas. For all incubation times, it is possible to observe that on HA + 1.5%BG surfaces cells tended to be more spread than on HA surfaces. It may also be observed that cells have preferentially chosen the grooves originated by the PLD coating process, to install themselves, so the proliferation is directioned along these grooves. This behaviour can be observed with more detail in Fig. 10 and is typical of osteoblastic cells, which need a surface to attach, grow, proliferate and differentiate.

Differences in cell proliferation on the HA and HA + 1.5%BG coatings, observed by SEM images, were confirmed through MTT (Fig. 7) and DNA (Fig. 8) results.

After 8 days, the MTT mean value for the HA + 1.5%BG coating is statistically equal to the control (polystyrene wells of tissue culture plates), but different from the HA coating (hypothesis tests for the difference between means at 0.05 level of confidence and $n = 5$), representing the presence of a higher number of viable cells on the glass containing coating comparing with the hydroxyapatite coating.

Results of the DNA analysis performed on testing samples and control exhibit a behaviour similar to the one found in MTT: an exponential growth tendency until day eight (end of experiment) for both PLD coatings and control (Fig. 8). After 2 days of contact, DNA content of the control samples became statistically different (t-test at 0.05 level of confidence and $n = 8$) comparing to the PLD coating samples for all contact times.

Due to inherent problems associated with the DNA quantification technical procedure, values obtained for all samples at 8 days (represented with dashed lines) are estimated to represent only 50% of the real DNA values. As referred before, calibration curves were established for both MTT and DNA quantification methods using MG63 suspensions of known cell numbers. The bis-benzimide DNA method isn't linear in all its range of application and two calibration curves have to be constructed, using reagents solutions of different concentrations. By definition MTT values are associated to viable (living) cells, while DNA content can be directly compared to the existing (total) number of cells. As a rule, a correlation between experimental values of DNA and MTT of 1.5–1.6 for PLD samples (and of 1.2 for polystyrene control) was observed, except for the DNA values at 8 days and, obviously, there could not be a higher number of viable cells than of total cells. Insufficient amount of sample prevented repetition of analysis using reagent solutions and calibration curve for higher concentrations region.

Another observation should be taken into consideration when analysing DNA results, especially when comparing results of the control with those of the PLD samples: disruption of cells with Triton was performed directly on the

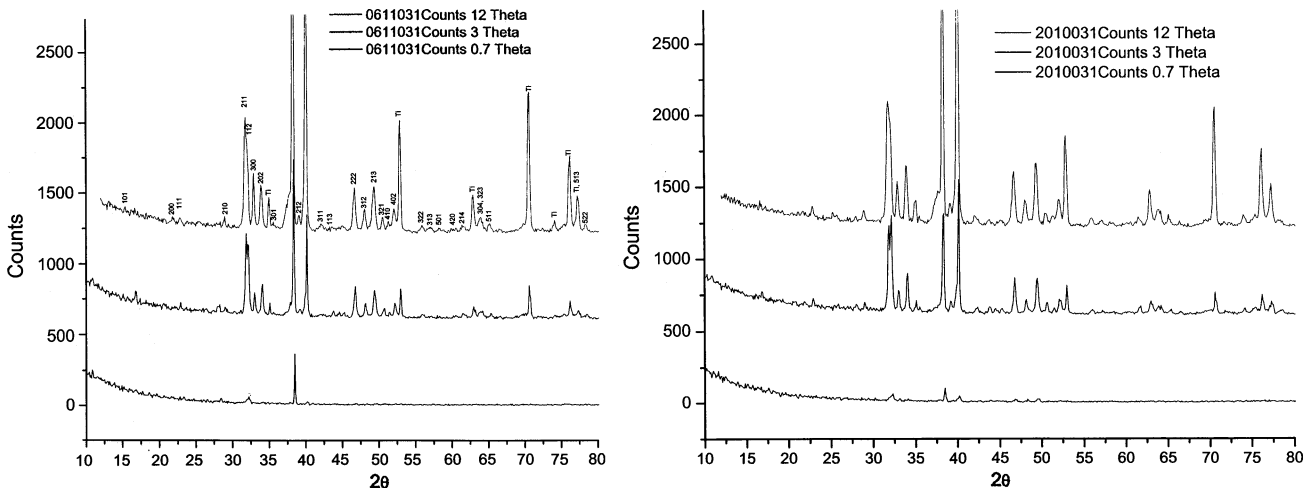

Fig. 5 XRD spectra of HA (left) and HA + 1.5%BG (right) PLD coatings after 48 h SBF immersion

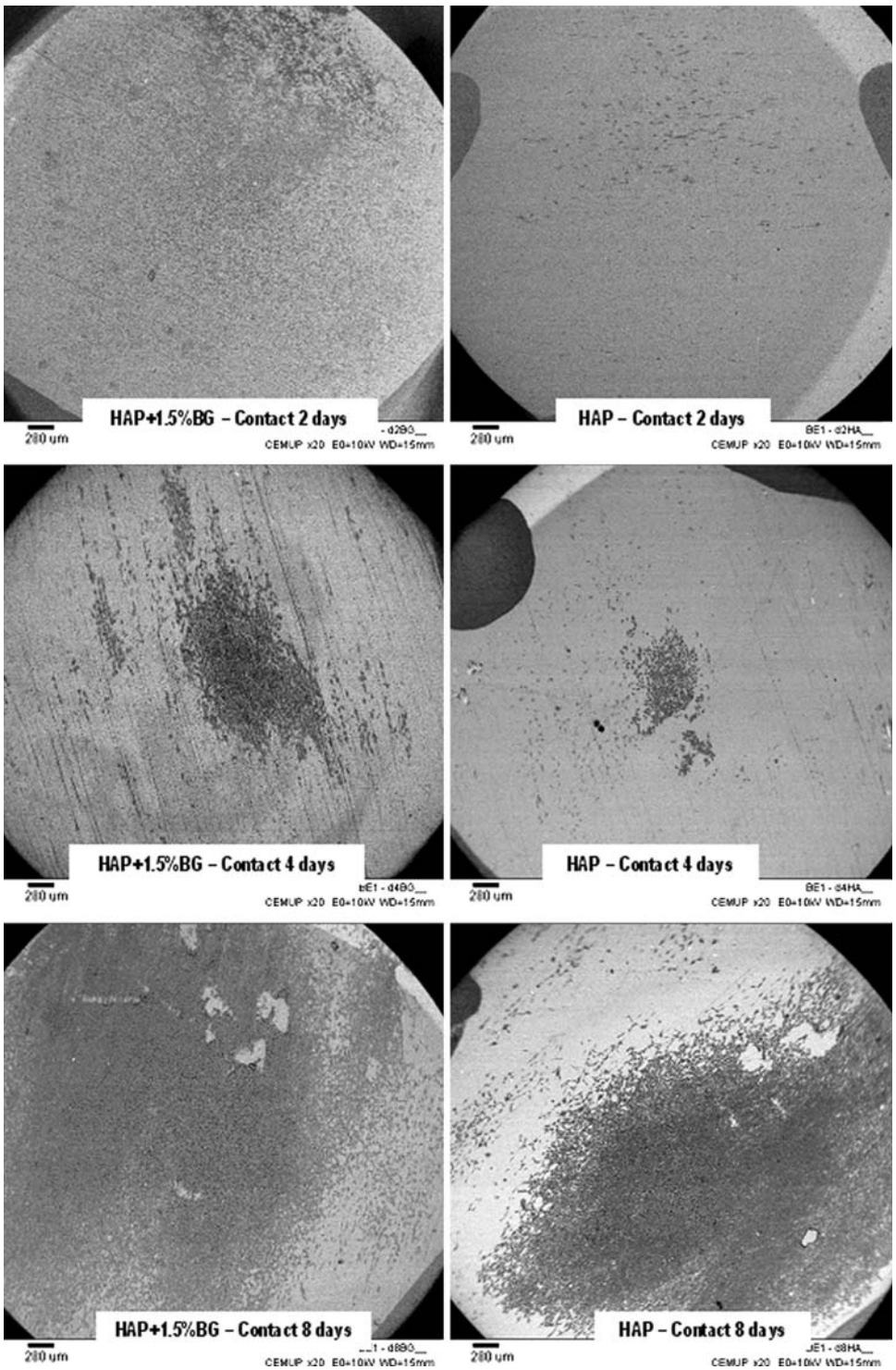

Fig. 6 SEM images of PLD coating discs (ϕ 6 mm) showing MG63 cell proliferation at different contact time (magnification 20×; energy 10 KV, backscattered electron mode)

samples (PLD) or on the wells (for the polystyrene control) to avoid excessive manipulation of samples and possible loss of material. It is likely that the rough surface of PLD samples could be favourable to settling or even adsorption of the cell lysate which wouldn't happen on a smooth plain surface like polystyrene, contributing to diminishing values.

MG63 cells morphology and contact with testing samples can be observed in SEM images of Figs. 9 and 10. In all images, is possible to observe, polygonal cells, overlaying each other, with a great number of cytoplasmatic extensions establishing contact with other cells and also providing cell fixation and attachment to the substrate. Other characteristics can be distinguished: many filipodia

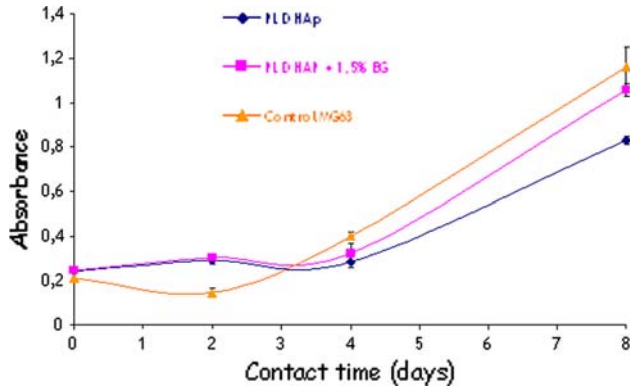

Fig. 7 Evolution with incubation time of the MTT assay results (absorbance at 540 nm) for the tested PLD coatings (HA and HA + 1.5%BG) and control (polystyrene)

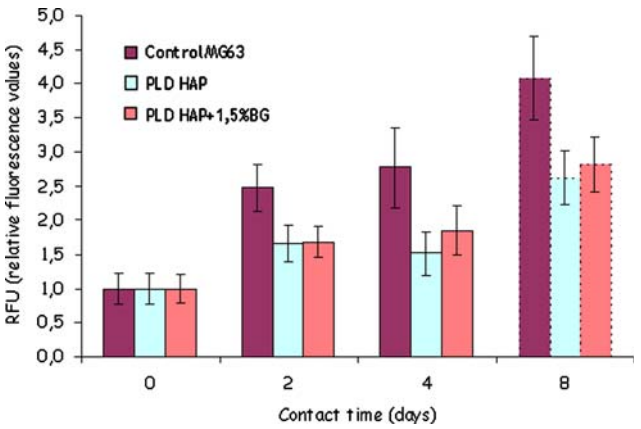

Fig. 8 DNA content (expressed as RFU values) of MG63 cells incubated on PLD coatings and control (polystyrene)

and ruffled cell surfaces are also typical of metabolically active osteoblasts.

Cells grown on HA + 1.5%BG coatings present a larger volume and a greater number of filipodia and cytoplasmatic extensions, few round cells (probably beginning cytoplasmatic division) and many precipitate agglomerates can also be observed. On HA coatings, cells presented themselves more flattened and overlapping. In both cases cells appear to prefer the surface grooves and other topographical irregularities to cling to.

4 Discussion

The observed homogeneous columnar structures of CaP PLD films, independently of the coatings' chemical composition is in agreement with results previously found by [12].

This immersion films morphology is very different from the ones found with plasma sprayed coatings or biomimetic processes that present a typical cauliflower and droplet morphology of agglomerated precipitate salts. This is also distinct from the morphology obtained with other coating techniques such as electrochemical deposition [31], vacuum plasma sprayed [32], sol-gel deposition [33] or even using other PLD techniques [34, 35] but similar to HA PLD coatings as reported by Clèries [36].

The PLD original coatings (not submitted to SBF immersion) thickness were 10 ± 2 μm, which is a consequence of the chosen PLD operating conditions including long ablation times. Despite poor solubility of hydroxyapatite and hydroxyapatite compounds in neutral solutions as SBF, during immersion, PLD films are subjected to dissolution and re-precipitation processes, possibly modifying their original structure. The values presented in Fig. 2 represent only the thickness of the detached layers exposed cross section and not the total film thickness. The magnitude and evolution, with immersion time, of these layer thickness values lead to the conclusion that these mechanically detached layers represent the part of the PLD film interacting with the SBF solution being

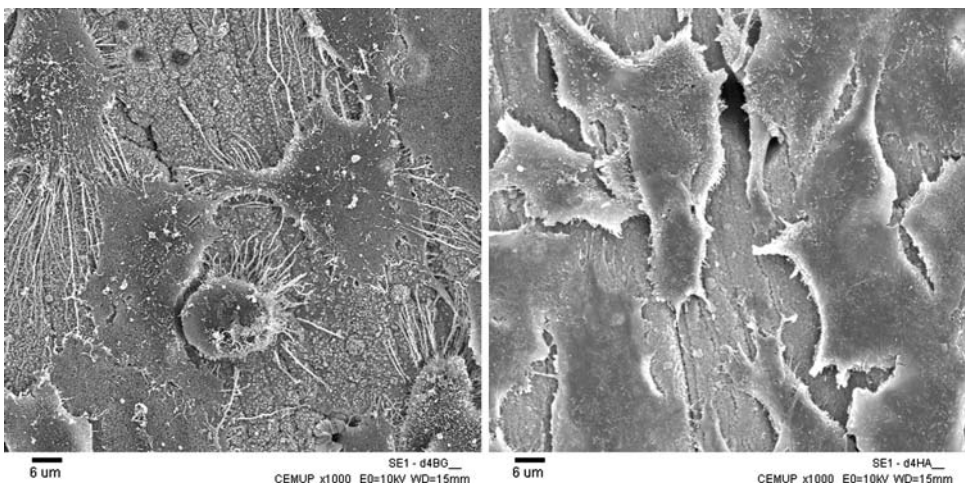

Fig. 9 SEM images of MG63 cells on HA + 1.5%BG (left) and HA (right) PLD coatings after 4 days of contact (magnification 1000×; energy 10 KV, secondary electron mode)

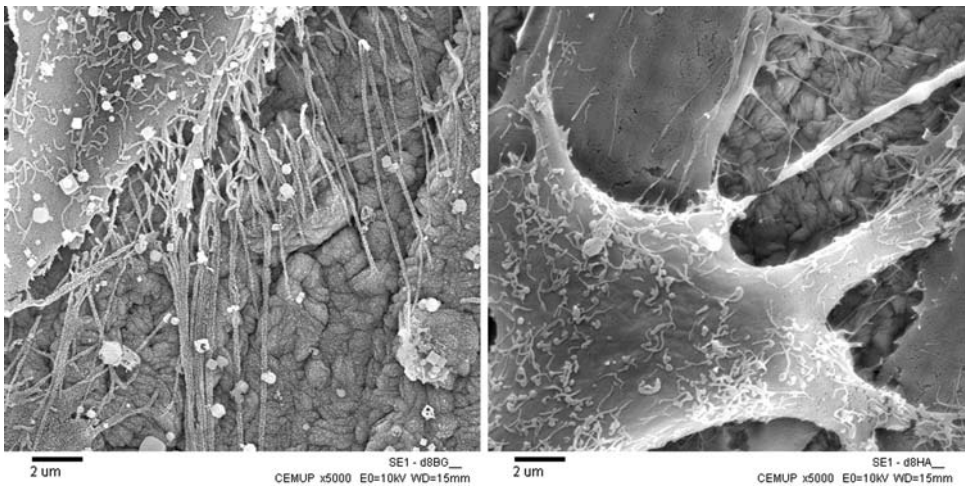

Fig. 10 SEM images of MG63 cells on HA + 1.5%BG (left) and HA (right) PLD coatings after 8 days of contact (magnification 5000×; energy 10 KV, secondary electron mode)

simultaneously dissolved and enlarged by precipitation. As a consequence, thicker detached layers in the HA + 1.5%BG coating indicates that this group of samples have undergone faster dissolution and re-precipitation processes, as expected, being in agreement with previous results [12] and also with AFM results, presenting also increased film roughness.

The inclusion of the glass improved the solubility of the hydroxyapatite film, and seemed to be responsible for a faster dissolution and re-precipitation process on the film surface during SBF immersion, leading to precipitation of apatite to a great extent in the case of HA + 1.5%BG coatings. Other studies involving SBF immersion of several calcium phosphate PLD coatings [27] demonstrated higher precipitation rates with $\beta\alpha$-TCP coatings, which is attributed to higher solubility of the TCP when compared to HA. Studies involving plasma sprayed glass/HA composites [37] have also demonstrated that the presence of the glass in the coating induced a faster surface CaP layer formation during SBF immersion as a consequence of a faster ion exchange of Ca^{2+} and PO_4^{3-} between the SBF solution and the tested materials.

XPS analyses showed no differences in the chemical composition of the PLD films surface after immersion in SBF and the Ca/P ratio tended to stabilize at 1.44, which is approximating the ratio of 1.49, typical of natural bone apatite, a calcium deficient carbonated apatite. Carbonated apatite (cHA) may result from the incorporation of CO_3^{2-} and Mg^{2+} as substituting impurity ions originated from the physiological fluids or SBF solution as reported by several authors [38–40].

Both SEM and AFM results indicate that the layers precipitated during SBF immersion replicated the original morphology of the PLD coating, probably as a consequence of a substituting precipitation process where Na^+ and Mg^{2+} (originated from SBF) were substituting calcium ions and CO_3^{2-} (also originated from SBF) were substituting for PO_4^{3-} and OH^- sites on the hydroxyapatite structure, as suggested by XPS results analysis and also by several authors [40, 41].

Hydroxyapatite is insoluble in water and salt solutions of pH values higher than 4.2; SBF solution, with the physiologic pH of 7.2, is supersaturated in Ca^{2+} and PO_4^{3-} relatively to HA. The driving force caused by concentration gradients promotes the precipitation of ions from the solution towards the surface, which is also the basic principle of biomimetic processes. However this tends towards a dynamic equilibrium, at a microscale, between the surface and the surrounding solution. XPS results demonstrate that, effectively during the initial hours of immersion, Ca and P atomic concentration at the PLD film surface diminished, until stabilization, while Mg and Na atomic concentrations increased, also until stabilization (data not shown).

Surface topography has been associated with mediation mechanisms involving protein adsorption (such as fibronectin and collagen) and consequent cellular response [26, 32, 42–44]. Studies with pure Ti implants, polished or treated to increase roughness, have demonstrated that cell proliferation and differentiation are surface roughness dependent. With these non-coated titanium implants, cell proliferation decreases and differentiation is enhanced on microrougher surfaces [25, 26]. Other studies using Ti6Al4V [45] or vacuum plasma sprayed titanium [32] samples in contact with MG63 cells confirmed these results and, besides demonstrating improvement in cell differentiation by phenotypic osteoblastic expression in moderately rough (3–5 μm Ra) surfaces. Also, it is commonly accepted that roughened surfaces can provide better mechanical interlocking with the host bone and consequently improve implant mechanical stability. However, very rough metallic surfaces may facilitate corrosion and crack initiation leading to reduced fatigue resistance of the implant and all associated consequences. On the other hand, too rough

(higher than 50 μm Ra) or too smooth surfaces (lower than 0.1 μm Ra) have similar effects on cellular response because surface topography is either too big or too small to be recognized by cells. These detect and respond most strongly to surface features with dimensions that approach the order of magnitude of the cell size. PLD films, obtained in the same conditions as in this work, present low roughness values (0.2–0.4 μm Ra), which are comparable to pre-treated pure titanium surfaces roughness. Results of cytocompatibility tests with MG63 cells performed in this work are in agreement with other authors conclusions, i.e., on HA + 1.5%BG PLD film cells spread and grow more extensively than on HA PLD coating. Furthermore, cells in contact with the former coating presented more characteristic structural features of osteoblasts than those grown on hydroxyapatite coatings. Remarkably, SBF immersion improved HA + 1.5%BG coating roughness to double the value of the HA film; and as there were no other differences between the two films after SBF immersion, it is reasonable to believe that the changes found in cellular behaviour may be attributed to the surface topography.

5 Conclusions

Bioactive CaP ceramic PLD coatings provide thin films with desirable characteristics for dental or orthopaedic applications. Thin films obtained with this technique are adherent and show uniform roughness throughout the surface.

Results obtained in this work have shown that these ceramic PLD films closely reproduce the surface topography of their metallic substrates, presenting a well-organised and compact columnar structure. This typical structure has shown not to be dependent on the chemical composition slight differences of the coatings, confirming previous results. Dissolution and re-precipitation phenomena took place during immersion in SBF, but they did not affect the columnar structure shown in the laser ablation films. However, the inclusion of a $CaO–P_2O_5$ bioactive glass, mixed with HA, in the PLD coating, increased surface roughness and columnar density when compared to pure hydroxyapatite PLD coating.

After contact with osteoblast-like cells (MG63), PLD coated samples exhibited very good acceptance and cytocompatibility when compared to control samples, where cells were grown on polystyrene.

MG63 cells showed good adhesion to PLD CaP coatings preferably "choosing" surface valleys or grooves to adhere and proliferating along the valley directions. Regarding cellular morphology, PLD samples cells presented typical features of osteoblasts, with many cytoplasmatic extensions, granular structures and filipodia, making contact with neighbouring cells and with surface irregularities. Comparing cell proliferation on HA + 1.5%BG and pure HA coatings, the former achieved higher values of cellular proliferation and the typical osteoblastic characteristics were more evident. These results are attributed to the differences found in the topography of both coatings, as in agreement with previous results cells prefer surfaces with moderate roughness, as in the case of the HA + 1.5%BG PLD coating. The SBF immersion films obtained over both PLD coatings did not show chemical or crystallinity differences.

References

1. L. L. HENCH, *J. Am. Ceram. Soc.* **74** (1991) 1487
2. L. L. HENCH, *Biomaterials* **19** (1998) 1419
3. S. H. PARK, A. LLINÁS, V. K. GOEL and J. C. KELLER, in "The Biomedical Engineering Handbook", Edited by: J. D. BRONZINO (CRC Press, LLC, Boca Raton, 2000)
4. L. L. HENCH, in "7th International Symposium on Ceramics in Medicine", Edited by: Ö. H. A. A. Y. URPO (Butterworth-Heinemann Ltd Oxford, England, 1994) p. 3
5. T. KOKUBO, *Biomaterials* **12** (1991) 155
6. H. AOKI, in "Science and Medical Applications of Hydroxyapatite" (JAAS Takayan Press. Ishiyaku euroAmerica, Inc., Tokyo, 1991) p. 6
7. V. P. ORLOVSKII, V. S. KOMLEV and S. M. BARINOV, *Inorg. Mater.* **38** (2002) 973
8. S. M. KENNY and M. BUGGY, *J. Mater. Sci. Mat. Med.* **14** (2003) 923
9. J. D. SANTOS, J. C. KNOWLES, R. L. REIS, F. J. MONTEIRO and G. W. HASTINGS, *Biomaterials* **15** (1994) 5
10. J. D. SANTOS, R. L. REIS, F. J. MONTEIRO, J. C. KNOWLES and G. W. HASTINGS, *J. Mat. Sci. Mat. Med.* **6** (1995) 348
11. M. P. FERRAZ, M. H. FERNANDES, J. D. SANTOS and F. J. Monteiro, *J. Mater. Sci.: Mater. Med.* **12** (2001) 629
12. M. P. FERRAZ, F. J. MONTEIRO, D. GIÃO, B. LÉON, P. GONZALEZ, S. LISTE, J. SERRA, J. ÁRIAS and M. PEREZ-AMOR, *Key Eng. Mat.* **254–256** (2004) 347
13. A. E. PORTER, L. W. HOBBS, V. BENEZRA ROSEN, M. SPECTOR, *Biomaterials* **23** (2002) 725
14. H.-K. KIM, J.-W. JANG and C.-H. LEE, *J. Mater. Sci.: Mater. Med.* **15** (2004) 825
15. Y. HARADA, J.-T. WANG, V. A. DOPPALAPUDI, A. A. WILLIS, M. JASTY, W. H. HARRIS, M. NAGASE and S.R. GOLDRING, *J. Biomed. Mater. Res.* **31** (1996) 19
16. J. L. ARIAS, M. B. MAYOR, J. POU, B. LÉON and M. PÉREZ-AMOR, *Appl. Surf. Sci.* **154–155** (2000) 434
17. J. D. SANTOS, R. L. REIS, F. J. MONTEIRO, J. C. KNOWLES, G. W. HASTINGS, *J. Mater. Sci.: Mater. Med.* **7** (1996) 187
18. J. L. ARIAS, M. B. MAYOR, J. POU, Y. LENG, B. LÉON and M. PÉREZ-AMOR, *Biomaterials* **24** (2003) 3403
19. J. L. ARIAS, M. B. MAYOR, J. POU, B. LÉON and M. PÉREZ-AMOR, *Appl. Surf. Sci.* **182** (2002) 448
20. J. L. ARIAS, M. B. MAYOR, J. POU, B. LÉON and M. PÉREZ-AMOR, *Vaccum* **67** (2002) 653
21. J. L. ARIAS, F. J. GARCIA-SANZ, M. B. MAYOR, S. CHIUSSI, J. POU, B. LÉON and M. PÉREZ-AMOR, *Biomaterials* **19** (1998) 883
22. M. B. MAYOR, J. L. ARIAS, S. CHIUSSI, F. GARCIA, J. POU, B. LÉON and M. PÉREZ-AMOR, *Thin Solid Films* **317** (1998) 363

23. T. KOKUBO, H. KUSHITANI, S. SAKKA, T. KITSUKI and T. YAMAMURO, *J. Biomed. Mater. Res.* **24** (1990) 721
24. F. J. MONTEIRO, M. P. FERRAZ, D. GIÃO, B. LEON, P. GONZALEZ, S. LISTE, J. SERRA and M. PEREZ-AMOR, in "17th European Conference on Biomaterials", Edited by: E. S. F. *Biomaterials* (Barcelona, Spain, 2002) p. P65
25. S. LOSSDÖRFER, Z. SCHWARTZ, L. WANG, C. H. LOHMANN, J. D. TURNER, M. WIELAND, D. L. COCHRAN and B. D. BOYAN, *J. Biomed. Mater. Res* **70A** (2004) 361
26. S. R. BANNISTER, C. H. LOHMANN, Y. LIU, V. L. SYLVIA, D. L. COCHRAN, D. D. DEAN, B. D. BOYAN and Z. SCHWARTZ, *J. Biomed. Mater. Res.* **60** (2002) 164
27. L. CLERIES, J. M. FERNANDEZ-PRADAS, G. SARDIN and J. L. MORENZA, *Biomaterials* **19** (1998) 1483
28. D. DE SANTIS, C. GUERRIERO, P. F. NOCINI, A. UNGERSBOCK, G. RICHARDS, P. GOTTE and U. ARMATO, *J. Mater. Sci.: Mater. Med.* **7** (1996) 21
29. C. KNABE, F. KLAR, R. FITZNER, R. J. RADLANSKI and U. GROSS, *Biomaterials* **23** (2002) 3235
30. F. GARCIA, J. L. ARIAS, M. B. MAYOR, J. POU, I. REHMAN, J. KNOWLES, S. BEST, B. LÉON, M. PÉREZ-AMOR and W. BONEFIELD, *J. Biomed. Mater. Res. (Appl. Biomater)* **43** (1998) 69
31. P. PENG, S. KUMAR, N. H. VOELCKER, E. SZILI, R. S. C. SMART and H. J. GRIESSER, *J. Biomed. Mater. Res.* **76A** (2006) 347
32. V. BORSARI, G. GIAVARESI, M. FINI, P. TORRICELI, A. SALITO, R. CHIESA, L. CHIUSOLI, A. VOLPERT, L. RIMONDINI and R. GIARDINO, *J. Biomed. Mater. Res. Part B: Appl. Biomater.* **75B** (2005) 359
33. C. MASSARO, M. A. BAKER, F. COSENTINO, P. A. RAMIRES, S. KLOSE and E. MILELLA, *J. Biomed. Mater. Res.* **58** (2001) 651
34. A. BIGI, B. BRACCI, F. CUISINIER, R. ELKAIM, M. FINI, I. MAYER, I. N. MIHAILESCU, G. SOCOL, L. STURBA and P. TORRICELLI, *Biomaterials* **26** (2005) 2381
35. H. ZENG and W. R. LACEFIELD, *J. Biomed. Mater. Res.* **50** (2000) 239
36. L. CLÈRIES, J. M. FERNANDEZ-PRADAS and J. L. MORENZA, *Biomaterials* **21** (2000) 1861
37. M. P. FERRAZ, F. J. MONTEIRO and J. D. SANTOS, *J. Biomed. Mater. Res.* **45** (1999) 376
38. P. LI and P. DUCHEYNE, *J. Biomed. Mater. Res.* **41** (1998) 341
39. J. WENG, Q. LIU, J. G. WOLKE, X. ZHANG and K. DE GROOT, *Biomaterials* **18** (1997) 1027
40. A. C. TAS, *Biomaterials* **21** (2000) 1429
41. T. KOKUBO, H.-M. KIM and M. KAWASHITA, *Biomaterials* **24** (2003) 2161
42. J.-L. DEWEZ, A. DOREN, Y.-J. SCHNEIDER and P. G. ROUXHET, *Biomaterials* **20** (1999) 547
43. K. ANSELME, P. LINEZ, M. BIGERELLE, D. LE MAGUER, A. LE MAGUER, P. HARDOUIN, H. F. HILDEBRAND, A. IOST and J. M. LEROY, *Biomaterials* **21** (2000) 1567
44. A. OKUMURA, M. GOTO, T. GOTO, M. YOSHINARI, S. MASUKO, T. KATSUKI and T. TANAKA, *Biomaterials* **22** (2001) 2263
45. H. J. KIM, S. H. KIM, M. S. KIM, E. J. LEE, H. G. OH, W. M. OH, S. W. PARK, W. J. KIM, G. J. LEE, N. G. CHOI, J. T. KOH, D. B. DINH, R. R. HARDIN, K. JOHNSON, V. L. SYLVIA, J. P. SCHMITZ and D. D. DEAN, *J. Biomed. Mater. Res.* **74A** (2005) 366